doi:10.14311/ppt.2017.1.95
Plasma Physics and Technology **4**(1):95–98, 2017

INVESTIGATION ON THE INFLUENCE OF GAS PRESSURE ON CO_2 ARC CHARACTERISTICS IN HIGH-VOLTAGE GAS CIRCUIT BREAKERS

Z. Guo, X. Li*, Y. Zhang, X. Guo, J. Xiong

State Key Laboratory of Electrical Insulation and Power Equipment, Xi'an Jiaotong University, Xi'an 710049, China

* xwli@mail.xjtu.edu.cn

Abstract. CO_2 is identified as a promising alternative gas of SF_6. The magnetohydrodynamics (MHD) arc model is established for a CO_2 circuit breaker. The influence of gas pressure is studied. The simulations are carried out for 0.5 MPa, 0.7 MPa and 0.9 MPa absolute filling pressure, allowing predictions of pressure and temperature distributions. The arc time constant θ and the power loss coefficient Q is extracted. The thermal interruption capability is estimated to grow with increasing filling pressure.

Keywords: CO_2, gas pressure, circuit breaker, Mayr equation.

1. Introduction

SF_6 is currently widely used in high-voltage gas circuit breakers because of its high dielectric strength and excellent arc interruption properties [1]. However, SF_6 is found to have extremely high global warming potential (approximately 23900 times that of CO_2) [2]. Among the alternative gases of SF_6, CO_2 and its mixtures are considered as the promising options and there has been some real products filled with pure CO_2 gas[3, 4].

Although the interruption performance of CO_2 is inferior to SF_6, the gap might become smaller with optimization design of CO_2 circuit breakers based on improved understanding. When CO_2 gas is used as an arc-quenching medium in high-voltage switchgear, the gas pressure may be perhaps several atmospheric pressures. In this paper, the influence of the gas pressure on the interruption performance of the CO_2 circuit breakers is investigated.

2. Simulation model

A 252 kV puffer-type SF_6 circuit breaker with a short-circuit current interrupting capacity of 63 kA is employed in this paper. The dynamic arc behaviors are simulated by adopting a 2D axisymmetric MHD arc model, which takes account of the Joule heating, the electromagnetic effect (the Lorenz force), the radiation loss and the turbulence enhanced mass, momentum and energy transplant. The MHD model is introduced in detail in our previous paper [5].

The plasma medium is assumed to satisfy the conditions of the local temperature equilibrium (LTE) and local chemical equilibrium (LCE). The nozzle ablation process is not considered in this paper. The thermodynamic and transport properties of CO_2 are taken from the study of Tanaka [6]. The net emission coefficient of CO_2 is taken from the study of Billoux [7]. The simplified geometry and computational domain of the circuit breakers are presented in Fig1.

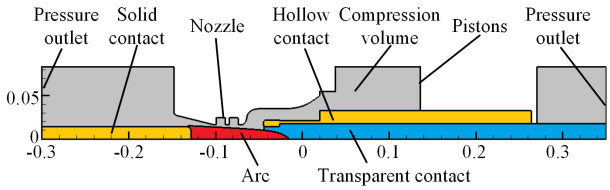

Figure 1. The simplified geometry and computational domain of the 252 kV puffer-type SF_6 circuit breakers

The commercial computational software ANSYS FLUENT is used to model the circuit breaker and solve the governing equations. The boundary and initial conditions of the simulation model are listed as follows: (1) The circuit breakers are filled with pure CO_2 at an absolute pressure of 0.5 MPa, 0.7 MPa and 0.9 MPa; the initial temperature is set to 300 K; (2) The movement velocity of the moving contacts is piecewise linearized from the action characteristic experiment result; (3) The electric potential of the solid contact is set at zero; (4) The transparent contact hypothesis is adopted as in some papers; (5) The short-circuit current of 31.5 kA (50 Hz) rms and arcing time of 9.95 ms are adopted.

3. Temperature characteristics

The temperature distribution in the arc extinguish chamber is an important indicator of the interruption process. Fig. 2 shows the temperature distributions in the arc area at 0.5 ms before the current-zero with different filling pressures. The highest temperature is located at the exit of the compression volume. This is because that there is a stagnation zone at the exit of the compression volume where the cold gas from the compression volume gets separated into two parts. The temperature at the arc core increases with the in-

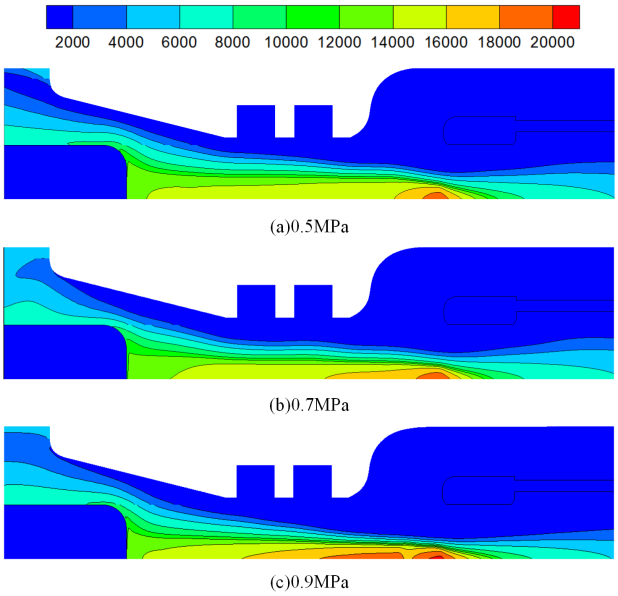

Figure 2. The temperature distributions in the arc area at 0.5 ms before the current-zero with different filling pressures. (Unit: K)

creasing filling pressure. The highest temperatures in the 0.5 MPa, 0.7 MPa and 0.9 MPa cases are 19.454 K, 19.803 K and 20.927 K.

Fig.3 describes the temperature distribution along the radial direction at the nozzle throat and at 0.5 ms before the current-zero with different filling pressures. It is clear that the temperature at the arc core becomes higher when the filling pressure is higher. However, the arc radius, defined as the position of the 4000 K isotherm in this paper as in some other papers, decreases with the increase of the filling pressure. What′s more, there is an inflection point on the radial temperature profile around 8000 K in each of the three cases. Fig.4 gives the distribution of C_P along the radial direction at the nozzle throat and at 0.5 ms before the current-zero with different filling pressures. Coincidentally, the inflection points on the temperature profiles corresponds well with the three peaks on the C_P profiles for each cases. The peak value of C_P here is caused by the dissociation of CO and will have detrimental effects on arc′s thermal recovery, because this effect will broaden the radiation reabsorption region and make the high temperature arc core less distinctive.

4. Pressure characteristics

Fig.5 gives the pressure distributions in the arc area at 0.5 ms before the current-zero with different filling pressures. There is a distinctive stagnation zone at the exit of the compression volume in each case, with an obvious high pressure region. In the 0.5 MPa case, an arresting shock wave occurs between the solid contact and the nozzle divergence cone. However, in the 0.7 MPa and 0.9 MPa cases, the shock wave at this

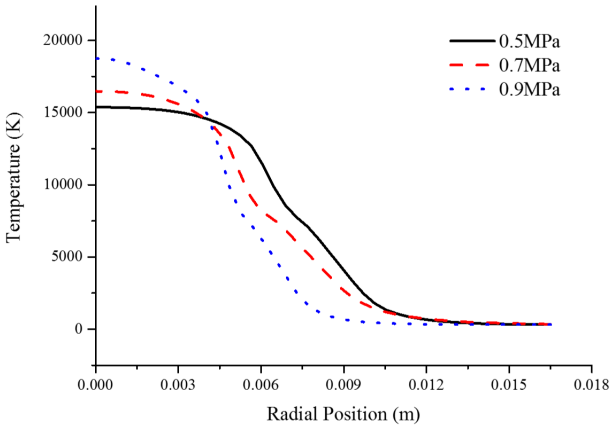

Figure 3. The temperature distribution along the radial direction at the nozzle throat (x=-0.07 m) and at 0.5 ms before the current-zero with different filling pressures.

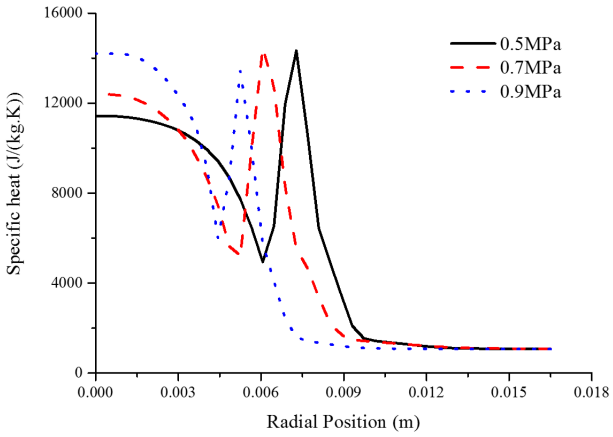

Figure 4. The distribution of the specific heat (C_P) along the radial direction at the nozzle throat (x=-0.07 m) and at 0.5 ms before the current-zero with different filling pressures.

location is much less stronger. Therefore, the filling pressure not only has an impact on the pressure values, but also affects the flow field during the interruption process. Besides, a slight shock wave also shows up inside the hollow contact in each case, which is caused by the contraction-expansion flow field structure.

5. Current zero characteristics

The arc time constant θ and the power loss coefficient Q are commonly used to evaluate the interruption capability of a circuit breaker, and generally give a believable result. Mayr equation is expressed as follow:

$$\frac{1}{g}\frac{\mathrm{d}g}{\mathrm{d}t} = \frac{1}{\theta}\left(\frac{u \cdot i}{Q} - 1\right) \tag{1}$$

Then the time constant θ and the power loss coefficient Q are expressed respectively:

$$\theta = \frac{g_1 i_2^2 - g_2 i_1^2}{i_1^2 \frac{\mathrm{d}g_2}{\mathrm{d}t} - i_2^2 \frac{\mathrm{d}g_1}{\mathrm{d}t}} \tag{2}$$

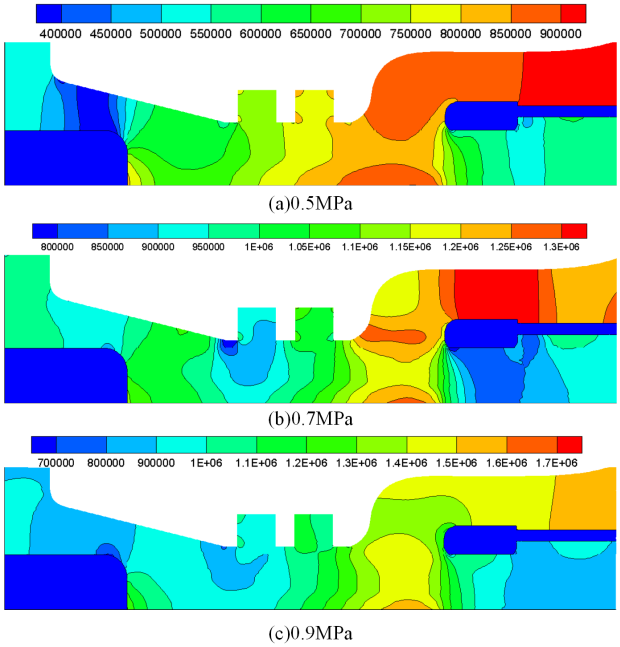

Figure 5. The pressure distributions in the arc area at 0.5 ms before the current-zero with different filling pressures. (Unit: Pa)

$$Q = \frac{i_2^2 \frac{\mathrm{d}g_1}{\mathrm{d}t} - i_1^2 \frac{\mathrm{d}g_2}{\mathrm{d}t}}{g_2 \frac{\mathrm{d}g_1}{\mathrm{d}t} - g_1 \frac{\mathrm{d}g_2}{\mathrm{d}t}} \tag{3}$$

In this paper, we assume that the time constant θ and the power loss coefficient Q keep constant within a simulation time step. Thus, the values of θ and Q at a specific time can be obtained by using two adjacent time steps as the two points required in equation (2) and (3). By this means, the variation of θ and Q over time is available. The θ and Q at the current zero point are obtained and shown in Fig.6. With the increase of the filling pressure, the time constant doesn′t show much change with a value around 2.52 µs. However, the power loss coefficient seems to increase monotonically with the increasing filling pressure.

In order to qualitatively evaluate the interruption capability of the circuit breaker, the post-arc current is predicted by using Mayr equation based on the calculated data of θ and Q at the current zero point. The RRRV and relative di/dt are varied to find the interruption limit. The results for the 0.5 MPa case are shown in Fig.7 and Fig.8. In Fig.7, the relative di/dt is fixed as 1. In Fig. 8, the RRRV is set as 2 kV/µs. It is clearly seen that with increasing RRRV or relative di/dt, the post-arc current increases effectively, and when RRRV or relative di/dt is beyond the critical value, the current rises sharply and the arc re-ignition happens. The critical RRRV in the 0.5 MPa, 0.7 MPa and 0.9 MPa filling pressure cases is determined to be approximately 0.63 kV/µs, 0.74 kV/µs and 0.81 kV/µs respectively. The critical relative di/dt in the 0.5 MPa, 0.7 MPa and 0.9 MPa filling pressure cases is determined to be approximately 31

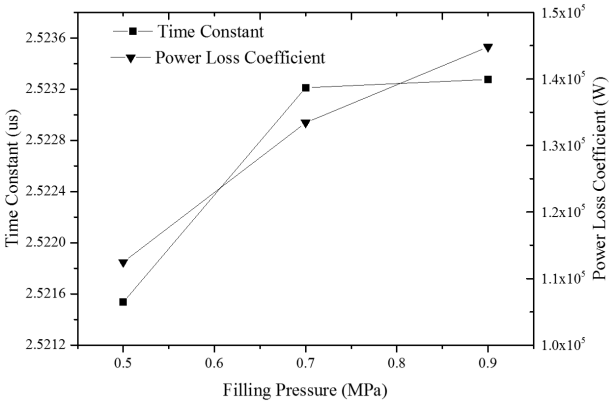

Figure 6. The time constant θ and the power loss coefficient Q at the current zero point with different filling pressures

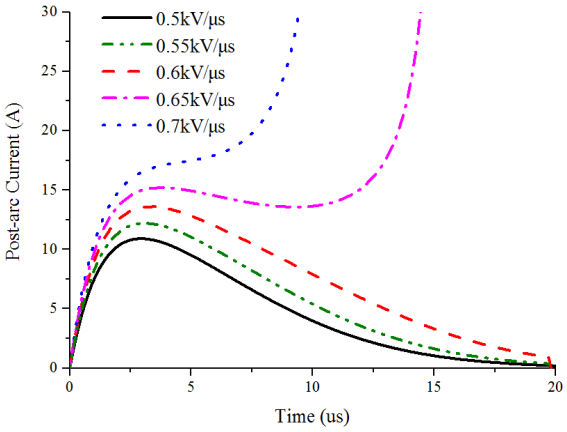

Figure 7. Variation of the post-arc current for different values of RRRV with the filling pressure of 0.7 MPa.

6. Conclusions

The performance of CO_2 gas as an interruption medium in high-voltage circuit breakers is investigated with different filling pressures. It is found that the highest temperature increases with the increasing filling pressure while the arc radius decreases with the increase of filling pressure. Besides, the arc temperature distribution has a close relationship with the specific heat (C_P) of the filling gas. The filling pressure not only has an impact on the pressure values, but also affects the flow field during the interruption process. The post-arc current is predicted by using Mayr equation based on the calculated data of θ and Q at the current zero point. For the 0.5 MPa, 0.7 MPa and 0.9 MPa filling pressure cases, the critical RRRV is determined to be 0.63 kV/µs, 0.74 kV/µs and 0.81 kV/µs and the critical relative di/dt is determined to be 31

Acknowledgements

The work was supported by National Natural Science Foundation of China (51607143, 51577143).

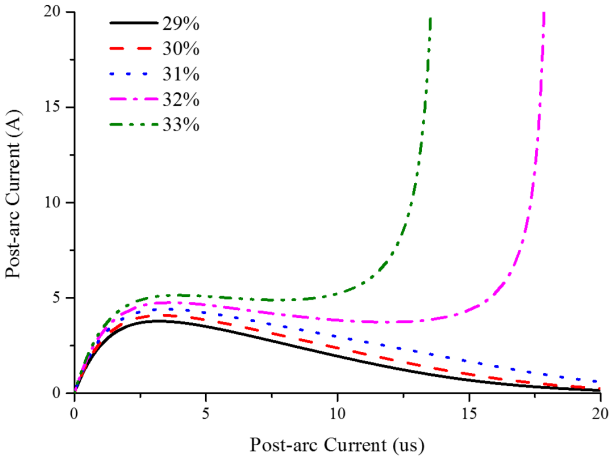

Figure 8. Variation of the post-arc current for different values of relative di/dt *with the filling pressure of 0.5 MPa.*

References

[1] J.O.L. Christophorou and R. Van Brunt. Sulfur hexafluoride and the electric power industry. *IEEE Electrical Insulation Magazine*, 13(20):5, 1997. doi:10.1109/57.620514.

[2] Y. Kieffel and F. Biquez. Sf6 alternative development for high voltage switchgears. *IEEE Electrical Insulation Conference*, pages 379–383, 2015.

[3] T. Uchii, T. Shinkai, and K. Suzuki. Thermal interruption capability of carbon dioxide in a puffer-type circuit breaker utilizing polymer ablation. *Transmission and Distribution Conference and Exhibition: Asia Pacific. IEEE/PES*, pages 1750–1754, 2002. doi:10.1109/TDC.2002.1177719.

[4] M. Seeger. Perspectives on research on high voltage gas circuit breakers. *Plasma Chemistry and Plasma Processing*, 35(3):527–541, 2015. doi:10.1007/s11090-014-9595-4.

[5] X. Jiang, X. Li, H. Zhao, and S. Jia. Analysis of the dielectric breakdown characteristics for a 252 kv gas circuit breaker. *Power Delivery IEEE Transactions on*, 28(3):1592–1599, 2013. doi:10.1109/TPWRD.2013.2254137.

[6] Y. Tanaka, N. Yamachi, S. Matsumoto, and M. Shibuya. Thermodynamic and transport properties of CO_2, CO_2–O_2, and CO_2–H_2 mixtures at temperatures of 300 to 30,000 K and pressures of 0.1 to 10 MPa. *Electrical Engineering in Japan*, 163(4):18–29, 2010. doi:10.1002/eej.20467.

[7] T. Billoux, Y. Cressault, V.F. Boretskij, A.N. Veklich, and A. Gleizes. Net emission coefficient of CO_2–Cu thermal plasmas: role of copper and molecules. *12th High-Tech Plasma Processes Conference*, page 2027, 2012. doi:10.1088/1742-6596/406/1/012027.